

Characterization of a Series of Far Red Absorbing Perylene Diones: A New Class of Fluorescent Probes for Biological Applications

Nectarios Klonis,^{1,3} Huiqin Wang,^{1,3} Nurul H. Quazi,^{2,3} Joanne L. Casey,^{1,3} Gregory M. Neumann,^{1,3} Dean R. Hewish,^{3,4} Andrew B. Hughes,^{2,3} Les W. Deady,^{2,3} and Leann Tilley^{1,3,5}

Received March 11, 2000; revised July 19, 2000; accepted July 24, 2000

The far red region of the spectrum is increasingly being utilised in many applications in the biosciences. However, apart from the cyanine group of dyes, there are relatively few far red fluorescent probes available which are of practical use. We have synthesised and characterised a new class of far red fluorescent probes based on the perylene dione chromophore. The 2,10-disubstituted perylene diones possess broad absorption spectra (>90 nm bandwidths), large Stokes shifts (>60 nm) and quantum yields of up to 0.5 with a maximum absorption at 610–640 nm in organic solvents or in solutions of non-ionic detergents. A number of derivatives have been synthesised that can be used as membrane probes, as chromogenic substrates for alkaline phosphatase, and for the labelling of macromolecules such as proteins and DNA. These novel far red fluorophores have potential applications in diagnostic and research applications.

KEY WORDS: Fluorescent probes; perylene diones; membrane probe; fluorescence microscopy; flow cytometry.

INTRODUCTION

A large number of fluorescent dyes are available commercially for use in direct fluorescence labelling applications such as fluorescence microscopy and flow cytometry, or as chromogenic or fluorogenic substrates in enzyme-linked immunoassays. The application of fluorescent reagents in these assays has advantages of sensitivity and safety compared with colorimetric or

radioactive reagents. Fluorophores which absorb in the far red region of the spectrum have a further advantage in that they show little susceptibility to optical interference from biological samples, since most biological chromophores absorb and emit light at much lower wavelengths [1,2]. In addition, they can be used in combination with the small and inexpensive diodes and detectors that have been developed for the telecommunications industry [1–4].

Apart from the cyanine dyes [5–10] and the phycobiliproteins [11], few fluorescent probes which possess absorption maxima in the far red region have been developed for biological applications. The arylsulphonated cyanine dyes (Cy5 and Cy5.5), in particular, have found many uses in diagnostic [12,13] and fluorescence microscopy applications [14,15]. Cy5 and Cy5.5 probes have absorption wavelength maxima of 650 nm and 670 nm, respectively. It would be useful to also have available

¹ Department of Biochemistry, La Trobe University, Bundoora, 3083, Victoria, Australia.

² Department of Chemistry, La Trobe University, Bundoora, 3083, Victoria, Australia.

³ Cooperative Research Centre for Diagnostic Technologies, La Trobe University, Bundoora, 3083, Victoria, Australia.

⁴ CSIRO Health Sciences and Nutrition, Parkville, Australia, 3052.

⁵ To whom correspondence should be addressed. Fax: 61-3-94792467. E-mail: L.Tilley@latrobe.edu.au

chromophores with absorption maxima near 630 nm as these could be maximally excited with cheap and powerful He-Ne lasers as well as with 635 nm diode lasers. Chromophores which absorb in the 590–630 nm wavelength range are also optimised for procedures based on energy transfer from phycoerythrin [16].

The red-violet compound dibenzo[*a,j*]perylene-8,16-dione (Table 1) is reported to be fluorescent in organic solvents [17–19]. Although this compound has been studied previously for applications involving the reversible addition of O₂ to a photoresponsive compound [17,19–22], the far red absorbance and fluorescence of members of this class of compounds have not previously been explored. We have synthesised a series of perylene diones [23] for applications as sensitive far red fluorophores in biological assays. We present the spectroscopic characterisation of the compounds and demonstrate their potential in a number of different applications.

EXPERIMENTAL

Reagents

Triton X-100, IgG (sheep anti-rabbit), alkaline phosphatase (bovine intestinal mucosa), p-nitrophenyl phosphate (PNPP), dimyristoyl L- α -phosphatidylcholine (DMPC) and L- α -phosphatidyl choline (egg yolk) were from the Sigma Chemical Company (St. Louis, MO). The cyanine dye Cy5.5 was from Amersham Life Sciences (Pittsburgh, PA). 3,3'-diethylthiadicyanide iodide was from Acros Organics (New Jersey, USA). 5'-Aminolink oligonucleotide with the sequence GCA AAC AGC TAT GAC CAT G was synthesised by GeneWorks (Adelaide, Australia). Perylene dione derivatives were prepared using two separate synthetic routes as described by Deady *et al.* [23] and were stored vacuum desiccated at 4°C in the dark. The structures of the compounds are shown in Table I. All other reagents were of the highest grade available.

Spectroscopic Measurements

Stocks of the derivatives were prepared at a concentration of 1 mg/ml in dimethylsulphoxide (DMSO) except for 2,10-DPPD which was prepared in water containing 1% ammonia solution (vol/vol). Stocks were diluted into the appropriate solvent so that the concentration of co-solvent was <2% (vol/vol).

Absorption spectra were recorded on a Cary 1E UV-Visible spectrophotometer using 1 nm data intervals, 0.5 nm slit bandwidths and 0.2 sec integration times. Fluores-

cence spectra were recorded on a Perkin-Elmer LS-50B luminescence spectrometer containing a red sensitive R928 photomultiplier using 10 nm excitation and emission slit widths and 0.5 nm data intervals. Emission spectra were recorded using excitation wavelengths across the absorption band and were corrected for the wavelength-dependent artifacts of the instrument using correction factors supplied by the manufacturer. All spectroscopic measurements were performed at room temperature.

Maxima in absorption and emission spectra (λ_{\max}) were determined as the wavelength at which the first derivative of the spectrum was zero. Spectral bandwidths (BW) were calculated as the full-width at half maximum. Quantum yields (QY) were calculated from corrected emission spectra [24,25] using 3,3'-diethylthiadicyanide iodide in methanol as the reference:

$$QY_s = QY_r \frac{Area_s n_s^2 (1 - 10_{(-Abs_r)})}{Area_r n_r^2 (1 - 10_{(-Abs_s)})} \quad (1)$$

where n is the refractive index of the solvent, Abs is the absorbance of the sample at the excitation wavelength, Area is the integrated area under the emission spectrum and subscripts r and s refer to the reference and sample, respectively. The quantum yield of the reference (QY_r) is 0.33 [26].

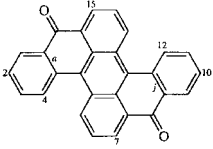
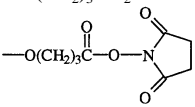
Fluorescence anisotropy measurements were recorded on a Hitachi 650-10S fluorescence spectrophotometer fitted with a polarization accessory. The excitation and emission wavelengths were 600 and 700 nm, respectively, with corresponding slit widths of 10 and 10–20 nm. An emission filter (Wratten gelatin filter No. 2A, Kodak) was employed to reduce the background signal. The temperature of the sample was controlled using a water bath and recorded with a temperature probe in the cuvette. The anisotropy (r) was calculated according to:

$$r = (I_{VV} - GI_{VH}) / (I_{VV} + 2GI_{VH}) \quad (2)$$

where I_{VV} and I_{VH} are the emission intensities recorded with the emission polariser in the vertical and horizontal orientations, respectively, following excitation with vertically polarised light, and G is an instrumental factor calculated as $G = I_{HV} / I_{HH}$, where I_{HV} and I_{HH} are the intensities recorded with the emission polariser in the vertical and horizontal orientations, respectively, following excitation with horizontally polarised light.

The susceptibility of the various compounds to photobleaching was quantitated by monitoring the loss of far red absorbance of samples exposed to the 633 nm line of a 35 mW He-Ne laser (Model 127, Spectra-Physics). Solutions (5 ml) with absorbance of 0.20–0.35 at 633

Table I. Structures of Dibenzo[*a,j*]Perylene-8,16-Dione and the Perylene Dione Derivatives Examined in this Study

Structure/functional group	Compound name	Abbreviation
	Dibenzo[<i>a,j</i>]perylene-8,16-dione	
–OCH ₃	2,4,10,12-Tetramethoxydibenzo[<i>a,j</i>]perylene-8,16-dione	2,4,10,12-TMPD
–OCH ₃	2,12-Dimethoxydibenzo[<i>a,j</i>]perylene-8,16-dione	2,12-DMPD
–OCH ₃	2,10-Dimethoxydibenzo[<i>a,j</i>]perylene-8,16-dione	2,10-DMPD
–OCH ₃	7,15-Dimethoxydibenzo[<i>a,j</i>]perylene-8,16-dione	7,15-DMPD
–OPO ₂ H ₂	2,10-(8,16-Dihydro-8,16 dioxodibenzo [<i>a,j</i>]perylene)diol bis(dihydrogen phosphate)	2,10-DPPD
–OH	2,10-Dihydroxydibenzo[<i>a,j</i>]perylene-8,16-dione	2,10-DHPD
–O(CH ₂) ₃ NH ₂	2,10-Bis-(3-Aminopropoxy) dibenzo[<i>a,j</i>]perylene-8,16-dione	2,10-DPAPD
	Di- <i>N</i> -Succinimidyl 4,4'-[2,10-(8,16-dihydro-8,16-dioxo) dibenzo[<i>a,j</i>]perylene]bis(oxy)]bisbutanoate	2,10-DSPD

nm were placed in 1.2 cm diameter glass tubes and irradiated from below.

Kinetics of Alkaline Phosphatase Hydrolysis of 2,10-DPPD and PNPP

The enzyme substrates, 2,10-DPPD and PNPP, were dissolved in 100 mM diethanolamine, 100 mM NaCl, pH 9.5 (DEA buffer). Aliquots (150 μ l) were added to multiple wells of a 96-well microplate and alkaline phosphatase (50 μ l, 0.002 units) was added to each well. The reaction was stopped by the addition of 2 M NaOH (50 μ l). Product formation was determined spectrophotometrically by monitoring the absorbance (*A*) at 750 and 405 nm for the 2,10-DPPD and PNPP substrates, respectively, using a Spectramax 250 (Molecular Devices) 96 well plate reader. Product formation (*P*) at each time was calculated according to:

$$P = (A - \epsilon_s S_o) / (\epsilon_p - \epsilon_s) \cdot V \quad (3)$$

where ϵ_p , and ϵ_s are the effective extinction coefficients of the product and substrate, respectively, and *V* is the reaction volume. To establish the nature of the product formed with 2,10-DPPD as a substrate, mass spectrometry was performed using a PE-Sciex API-300 electrospray ionisation mass spectrometer.

Conjugation of 2,10-DSPD to IgG and DNA

2,10-DSPD (200 nmol in 5 μ l DMSO) was added to the aminolink oligonucleotide (7 nmol) in 55 μ l 80

mM NaHCO₃. The reaction was allowed to proceed overnight at room temperature in the dark. The sample was centrifuged to sediment any undissolved dye and the supernatant was applied to a Sepharose 4B column (Pharmacia, Uppsala, Sweden) and eluted with PBS. The conjugate, possessing the far red absorbance of the perylene dione and the UV absorbance of the DNA, eluted prior to the total volume of the column. For mass spectroscopic analysis of the product, buffer exchange with 10 mM ammonium acetate was achieved by gel filtration. For labelling of protein, 2,10-DSPD (190 nmol in 10 μ l DMSO) was incubated overnight at room temperature with IgG (15 nmol) in 500 μ l 0.12 M NaHCO₃, 1% Triton X-100 (vol/vol) and purified using a 1 ml Protein G-Sepharose column (Pharmacia, Uppsala, Sweden).

Examination of 2,10-DPAPD and 2,10-DMPD as Membrane Probes

Small unilamellar vesicles (SUVs) were prepared fresh daily by drying egg yolk phosphatidylcholine or DMPC (13 μ mol in chloroform or methanol, respectively) under a stream of nitrogen and resuspending the lipid in PBS (1.5 ml) by vortexing. The suspension was placed in an ice-water bath (egg yolk phosphatidylcholine) or at $> 30^\circ\text{C}$ (DMPC), sonicated for twenty 30 second intervals with a Model XL2000 Microson Ultrasonic Homogeniser (Misonix, Farmingdale, NY) and centrifuged to sediment traces of titanium particles. DMPC SUVs were maintained at $> 30^\circ\text{C}$ until required. Perylene diones were added to the SUVs from stocks in methanol

so that the final methanol concentration was < 2% (vol/vol). For all measurements involving SUVs, appropriate corrections were made for light scattering utilising samples not containing probe.

Erythrocyte ghosts were prepared as described previously [27]. Perylene diones were added from stocks in DMSO to a 10% suspension of erythrocytes or ghosts and centrifuged to remove any unincorporated probe. A final molar ratio of about one probe molecule per 100 lipid molecules was achieved. Live mouse NS-1 myeloma cells (2×10^6 cells) were washed by centrifugation with PBS and incubated with 10 μg of 2,10-DPAPD at 37°C for 45 minutes. The cells were washed 2 times with PBS then resuspended in culture medium (Dulbecco's modified Eagle's medium plus 10% foetal calf serum) and cultured at 37°C.

Flow cytometric analysis was performed on a Coulter EPICS® Elite flow cytometer. Illumination of the bound dye was with a 10mW He-Ne laser at 633 nm. Red fluorescence was detected at 675 nm. Forward angle and 90 degree light scatter signals were recorded from illumination at 488 nm with an Argon ion laser. Data collection was triggered from the forward angle light scatter signal and red cell ghost fluorescence was gated on the main population of particles detected by light scatter. Confocal microscopy on red cell ghosts was performed using a Leica TCS-NT laser scanning confocal microscope, equipped with a krypton/argon laser using the 647 nm line. The confocal scan head was mounted on a Leica TCS microscope. For confocal microscopy of NS-1 cells, an Optiscan® F900e confocal scanning head was used, mounted on an Olympus BX60 microscope. Illumination was with a krypton/argon laser using the 568nm line and emission was observed at greater than 590nm.

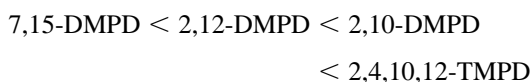
RESULTS

Spectral Properties and Stability of Perylene Dione Derivatives

The parent compound dibenzo[*a,j*]perylene-8,16-dione has an absorption maximum of 570 nm and an extinction coefficient of 23–29,000 $\text{M}^{-1}\text{cm}^{-1}$ in organic solvents [17,19], and forms a colourless endoperoxide when it is exposed to visible light in the presence of oxygen [17,19,21]. To examine the potential of the perylene dione class as probes for use in biological applications, we prepared a series of derivatives containing methoxy substituents at different positions on the ring structure (Table I) and examined the influence of the

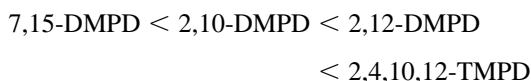
functional groups on the spectral properties and stability of the chromophore.

Each of the methoxy derivatives examined absorbs in the far red region of the spectrum and possesses a similar extinction coefficient in DMSO (19,000–25,000 $\text{M}^{-1}\text{cm}^{-1}$; Table II) to the parent chromophore. However, the absorption maxima exhibit a red shift up to 70 nm relative to the parent chromophore with the absorption maxima conforming to the following series:



The red shift is associated with a broadening of both the absorption and emission spectra, an increase in the Stokes shift, and a large decrease in quantum yield (Table II).

The photostability of the methoxy derivatives was examined by exposing them to the 633 nm line of a He-Ne laser. All the derivatives exhibit a decrease in absorbance over time (Fig. 1) which correlates with a decrease in their fluorescence (data not shown). Samples which were kept in the dark did not exhibit any absorbance loss (data not shown). The compounds exhibit an increasing stability in the order:



Since the spectral properties and stability of the 2,10- and 2,12-DMPD derivatives are similar, there is a good correlation between the above trends in the spectral properties and the stability of the various methoxy derivatives.

The absorption and emission spectra of 2,10-DMPD in DMSO are shown in Fig. 2, and the spectral properties of 2,10-DMPD in various solvents are summarised in Table III. The general structure of the absorption spectrum in similar in DMSO, chloroform and methanol although there are small changes in λ_{max} (blue shifts up to 10 nm relative to DMSO). However, the absorption spectrum in PBS is broader and contains a pronounced shoulder or second peak (Fig. 2, inset). This type of spectrum is also observed in the cyanine dyes and is attributed to the presence of non-fluorescent dimers or higher order aggregates [28–30]. Evidence that the perylene diones form aggregates in PBS also comes from gel filtration experiments in which the perylene diones are observed to elute in the void volume (data not shown).

The fluorescence of 2,10-DMPD is sensitive to solvent (Table III). The chromophore is highly fluorescent in chloroform (QY = 0.48) but shows a substantial decrease in fluorescence in the more polar/protic solvents, DMSO (QY = 0.29) and methanol (QY = 0.03). The reduction in the quantum yield is associated with a

Table II. Spectral Properties of Perylene Dione Derivatives in DMSO

Compound	Absorption			Emission		
	λ_{\max} (nm)	BW ^a (nm)	$\epsilon_{\lambda_{\max}}^{\text{IM}}$ ($\text{M}^{-1}\text{cm}^{-1}$)	Stokes shift (nm)	BW ^a (nm)	QY
2,4,10,12-TMPD	638	105	21,200	94	120	0.06
2,10-DMPD	617	94	21,800	64	111	0.29
2,12-DMPD	609	89	25,200	64	109	0.36
7,15-DMPD	586	74	19,400	29	82	0.82
2,10-DPPD ^b	617 ^c	133	9,000	76	117	0.02
2,10-DHPD	637	107	23,000	71	105	0.14
2,10-DPAPD	622	101	28,200	67	111	0.25
2,10-DSPD	623	97	29,600	63	110	0.26

^a Spectral bandwidth.

^b Compound possesses an extinction coefficient of $9,600 \text{ M}^{-1}\text{cm}^{-1}$ at 622 nm in water under basic conditions (0.01 M NaOH).

^c Spectrum exhibits double peak with other maximum at 588.

broadening of the emission spectrum and an increase in the Stokes shift. No fluorescence is observed from 2,10-DMPD in PBS. However, the compound is fluorescent in PBS in the presence of detergent (Table III).

The spectral properties of 2,10-DMPD in PBS in the presence of 1% Triton X-100 (vol/vol) approach those observed in chloroform and DMSO (Table III). This indicates that the chromophore is located in a less polar and protic environment presumably at the lipid-water interface or within the hydrophobic interior of the detergent micelle. The reduction in the absorption bandwidth

upon association further indicates that the chromophore is associated with the micelles in a “monomeric” or non-aggregated form. The photostability of 2,10-DMPD is increased when it is associated with Triton X-100 micelles compared to its stability in DMSO (Fig. 1). Indeed, under these conditions, the chromophore shows a lower susceptibility to photobleaching compared to Cy5.5 in PBS (Fig. 1).

A series of disubstituted derivatives containing various functional groups at the 2 and 10 positions were synthesised to examine their potential for use in different biological applications. The spectral properties of these derivatives in DMSO are compared in Table II. We make the following points regarding the effects of replacing the methoxy groups in the derivatives. Firstly, replacing the methoxy group with a propoxy-based group in the 2,10-DPAPD and 2,10-DSPD derivatives has little effect on the spectral properties of the chromophore. Secondly, substituting the methoxy group with a hydroxyl group, as in 2,10-DHPD, produces a 20 nm red shift and a 2-fold reduction in the quantum yield. Thirdly, the presence of the phosphate group in 2,10-DPPD results in a substantial reduction in the extinction coefficient and quantum yield. In addition, the absorption spectrum exhibits a double peak. This feature may reflect an aggregated state of this chromophore in DMSO (see above).

The 2,10-disubstituted derivatives show the same general trends in their spectral properties in various solvents as 2,10-DMPD. The exceptions are (i) the phosphate derivative, 2,10-DPPD, which is weakly fluorescent in PBS in the absence and presence of detergent (QY 0.004 and 0.01, respectively); and (ii) the hydroxy derivative, 2,10-DHPD, which under basic conditions in water exhibits a 100 nm red-shift in its absorption spectrum (Fig.

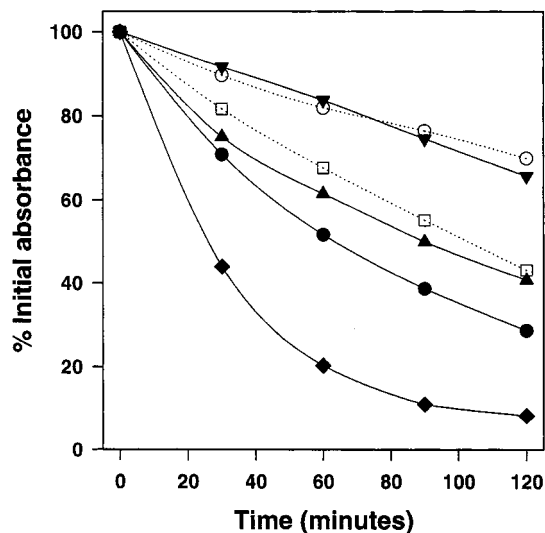


Fig. 1. Stabilities of 2,4,10,12-TMPD (\blacktriangledown), 2,12-DMPD (\blacktriangle), 2,10-DMPD (\bullet), 7,15-DMPD (\blacklozenge) in DMSO and 2,10-DMPD in PBS\1% Triton X-100 (\circ) upon exposure to He-Ne laser. The loss of far red absorbance upon exposure to light from a He-Ne laser was quantitated as described in Materials and Methods. The profiles are compared with that of Cy5.5 in PBS (\square).

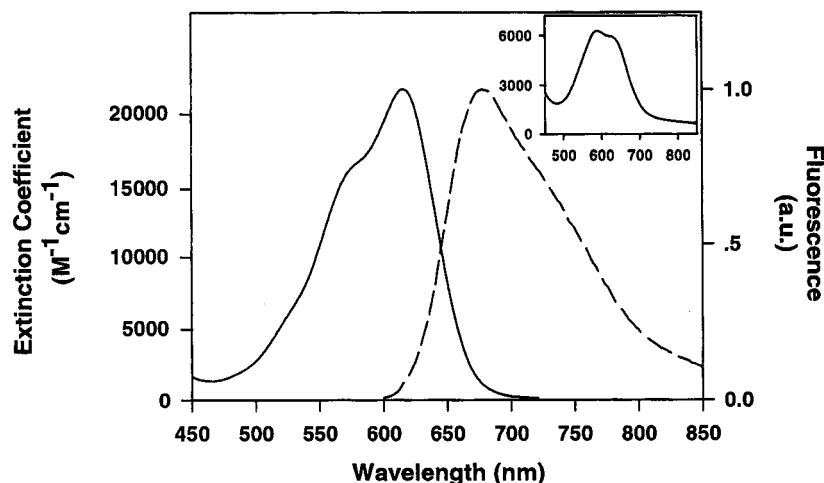


Fig. 2. Absorption (—) and emission spectra (---) of 2,10-DMPD in DMSO. Inset: Absorption spectrum of 2,10-DMPD in PBS.

3A) and is non-fluorescent even in the presence of detergent. The red-shift reflects the ionisation of the hydroxyl group(s) and occurs with a pKa of 9.5 (data not shown).

Potential Applications of 2,10-DPPD as an Alkaline Phosphatase Substrate

The ability of alkaline phosphatase to convert the phosphate derivative, 2,10-DPPD, to the hydroxy derivative, 2,10-DHPD, was examined, making use of the red shifted absorbance of the hydroxy derivative at alkaline pH. The absorption spectrum of a sample containing 2,10-DPPD exhibits a time-dependent change in the presence of alkaline phosphatase at pH 11 (Fig. 3B). The spectrum produced after extensive incubation with enzyme (Fig. 3B, solid line) resembles that of 2,10-DHPD under basic

conditions (Fig. 3A). This indicates that the time-dependent spectral change reflects the enzyme catalysed hydrolysis of the 2,10-DPPD substrate to form the 2,10-DHPD product. The removal of both phosphate groups by alkaline phosphatase was confirmed by negative ion mass spectrometric analysis (data not shown).

The kinetics of alkaline phosphatase hydrolysis of 2,10-DPPD were examined at pH 9.5. The enzyme activity was quenched at various times by the addition of NaOH and product formation was quantitated using the 750 nm absorbance, which is predominantly due to the ionised form of 2,10-DHPD under these conditions. As shown in Fig. 3C, the rate of product formation is linear and corresponds to the production of 0.07 μmol product/min/unit enzyme or 0.14 μmol phosphate/min/unit enzyme. This is comparable to the activity of the enzyme towards the PNPP substrate which it hydrolyses at a rate of 0.16 μmol phosphate/min/unit enzyme (Fig. 3C). However, the assay employing 2,10-DPPD as the substrate exhibits a 10-fold lower sensitivity for enzyme detection. This reflects the lower extinction coefficient of the product, and the significant absorbance of the substrate at the wavelength utilised in the assay (see Fig. 3A).

Fluorogenic substrates are commonly employed in alkaline phosphatase assays [31,32]. A fluorescence assay was developed which makes use of the large quantum yield of 2,10-DHPD in organic solvents. The assay was performed in a 96-well format using a two phase detection system where the fluorescent product is extracted into an equal volume (100 μl) of the organic phase (butanol). A time dependent increase in fluorescence intensity related

Table III. Spectral Properties of 2,10-DMPD in Various Solvents

Solvent	Absorption		Emission		QY
	λ_{max} (nm)	BW (nm)	Stokes shift (nm)	BW (nm)	
Chloroform	613	94	61	101	0.48
DMSO	616	94	64	111	0.29
Methanol	605	101	100	137	0.03
PBS	621 ^a	150	<i>nf</i>	<i>nf</i>	<i>nf</i>
PBS/Tx-100 ^b	613	101	67	117	0.08
PBS/SUVs ^c	611	98	61	111	0.10

^a Spectrum exhibits double peak with other maximum at 589 nm.

^b 2,10-DMPD in PBS in the presence of 1% Triton X-100 (vol/vol).

^c 2,10-DMPD (1 μM) in PBS in the presence of egg yolk phosphatidylcholine SUVs (1 mM). *nf*, no fluorescence detected.

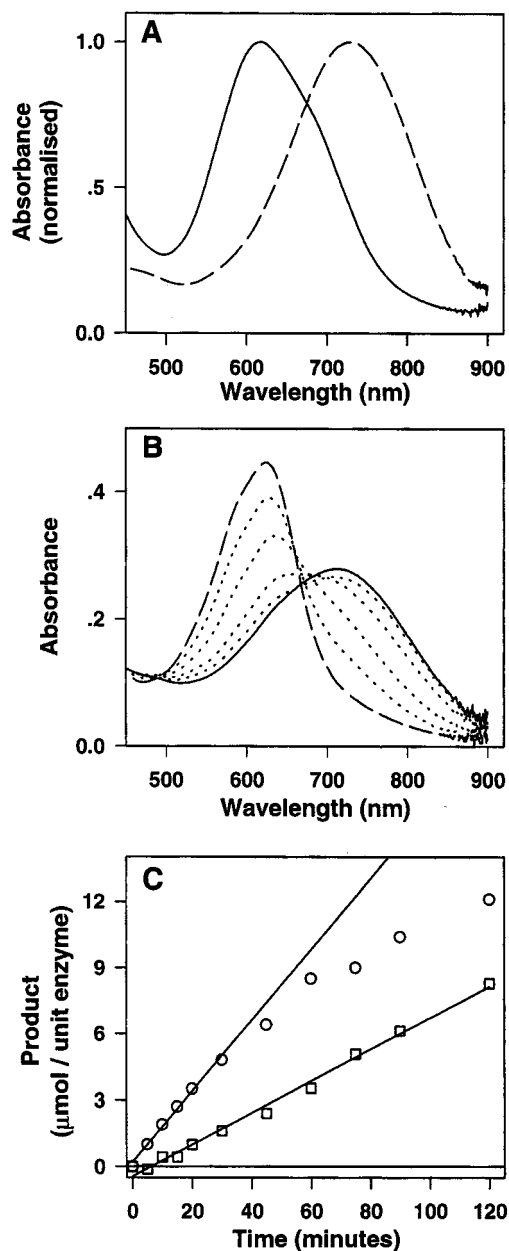


Fig. 3. 2,10-DPPD as a substrate for alkaline phosphatase. (A) Absorption spectrum of 2,10-DHPD in PBS (—) and in 0.01 M NaOH (---). (B) Effect of alkaline phosphatase on the absorption spectrum of a sample containing 2,10-DPPD at pH 11. The absorption spectrum of a 1 ml sample containing $46 \mu\text{M}$ 2,10-DPPD in 100 mM diethanolamine, 100 mM NaCl, 0.1 mg/ml albumin was recorded before (—) and 5, 15, 45 and 150 minutes after the addition of 1 unit of alkaline phosphatase (.....). The spectra show a progressive decrease in absorbance at 600 nm with time. An additional 35 units of enzyme was then added and the spectrum recorded following a 30 minute incubation (—). (C). Kinetics of alkaline phosphatase catalysed hydrolysis of 2,10-DPPD (\square) and PNPP (\circ). The enzyme (0.002 units) was added to the substrates ($540 \mu\text{M}$) in DEA buffer, pH 9.5. The absorbance was monitored over time and converted to μmol product as described in

to the amount of enzyme added was observed (data not shown).

Potential Applications of 2,10-DSPD for Covalent Labelling of Macromolecules

To assess the usefulness of the amino-reactive derivatives as fluorescent tags for proteins and DNA, IgG and aminolink oligonucleotide conjugates were prepared. The purified conjugates possess characteristic protein or DNA absorption in the UV region and perylene dione absorbance in the far red region (data not shown). The absorption spectra were used to estimate the molar ratio of perylene dione to macromolecule as 1:1 and 0.6:1 for the DNA and IgG conjugates, respectively. The quantitative labelling of the DNA and the 1:1 stoichiometry of the DNA conjugate were confirmed by positive ion mass spectrometric analysis (observed mass: 6553.4 ± 0.7 Da, expected mass: 6553.6 Da). The presence of conjugated IgG was confirmed by SDS-PAGE using 10% acrylamide under non-reducing conditions. This revealed the presence of a red fluorescent band under UV light which corresponded to the IgG band (data not shown).

The IgG-perylenone dione conjugate is not fluorescent in aqueous solution (PBS) or when immobilised onto a nitrocellulose membrane. The oligonucleotide-perylenone dione conjugate exhibits a weak fluorescence in PBS ($QY = 0.007$). Both compounds exhibit a weak fluorescence in PBS in the presence of 1% Triton X-100 ($QY = 0.01-0.02$).

Potential Applications of 2,10-DMPD and 2,10-DPAPD as Membrane Probes

The ability of the methoxy derivative, 2,10-DMPD, and the aminopropoxy derivative, 2,10-DPAPD, to interact with membranes and act as probes of the lipid environment was examined by titrating them with egg yolk phosphatidylcholine SUVs. The compounds exhibit a relatively rapid fluorescence increase when they are added to the SUVs as methanolic solutions, with greater than 80% of the fluorescence developed in the first five minutes. The increase in fluorescence is dependent on the phospholipid concentration (Fig. 4A). In the case of 2,10-DMPD, the fluorescence reaches a maximum

Materials and Methods. The lines represent the result of linear regression over the linear parts of the curves and possess slopes of 0.16 and 0.07 $\mu\text{mol product}/\text{min}/\text{unit enzyme}$ for the PNPP and DPPD substrates, respectively.

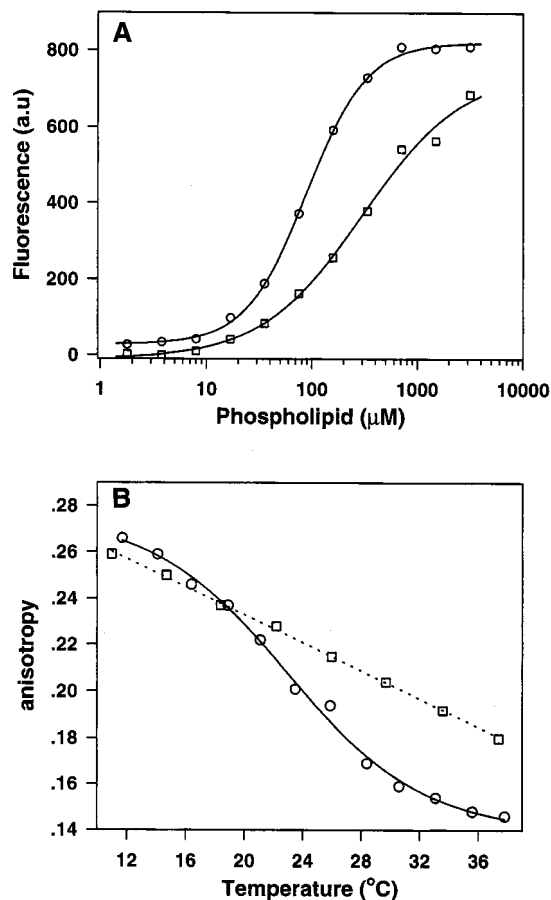


Fig. 4. 2,10-DMPD and 2,10-DPAPD as membrane probes. (A) Effect of phospholipid concentration on the fluorescence of 2,10-DMPD (\circ) and 2,10-DPAPD (\square). The probes ($1 \mu\text{M}$) were titrated with egg yolk phosphatidylcholine SUVs in PBS. (B) Effect of temperature on the fluorescence anisotropy of 2,10-DMPD ($1.2 \mu\text{M}$) in PBS in the presence of 1% Triton X-100 (\square) and 1 mM DMPC SUVs (\circ). The temperature was scanned from highest to lowest temperature.

intensity at a concentration of $700 \mu\text{M}$ phospholipid (lipid:probe $\sim 700:1$) with an apparent dissociation constant of $\sim 90 \mu\text{M}$ with respect to phospholipid. The fluorescence intensity of 2,10-DPAPD does not reach saturation even in the presence of 3.2 mM phospholipid (lipid:probe $\sim 3200:1$) indicating a much lower affinity of the interaction (apparent dissociation constant $> 300 \mu\text{M}$). This is consistent with the more polar 2,10-DPAPD having a greater solubility in the aqueous phase. The spectral properties of 2,10-DMPD associated with phospholipid SUVs are similar to those of 2,10-DMPD in the presence of detergent (Table III).

In addition to changes in intensity, the fluorescence anisotropy of 2,10-DMPD is also affected by its association with SUVs. The fluorescence anisotropy of 2,10-DMPD is low when it is present in chloroform (0.005

and exhibits a substantial increase (0.14–0.27) when it is in PBS in the presence of Triton X-100 or DMPC SUVs (Fig. 4B). This is consistent with the probe associating with the micelles and vesicles and thus having slower and/or more restricted rotational dynamics. The maximum anisotropy measured in this study (0.27) represents a lower limit estimate for the limiting anisotropy of the perylene dione chromophore.

The anisotropy in the presence of Triton X-100 shows a steady increase with decreasing temperature. In contrast, the anisotropy exhibits a sigmoidal dependence on temperature when the probe is associated with DMPC SUVs (Fig. 4B). A similar dependence is observed with the commonly used probes of membrane fluidity diphenylhexatriene [33,34] and the anthroyloxy fatty acid series [35]. The probe therefore appears to sense the phase transition of DMPC SUVs which occurs over the temperature range $14\text{--}27^{\circ}\text{C}$ with a mid-point at 21°C [34].

To determine whether 2,10-DMPD and 2,10-DPAPD might be useful as general membrane probes in cytometric applications, erythrocyte ghosts and intact erythrocytes were incubated with a small volume of the probe in DMSO, then subjected to flow cytometry. The background signal from the ghosts was very small and a large increase in the measured fluorescence intensity was observed upon addition of 2,10-DPAPD (Figs. 5A and B). The intact erythrocytes gave a higher background signal. However the addition of 2,10-DPAPD was again associated with a substantial increase in the fluorescence signal (Figs. 5C and D). Similar results were observed using 2,10-DMPD (data not shown).

Staining of live NS-1 myeloma cells with 2,10-DPAPD resulted in the acquisition of strong red fluorescence by the cells (Figs. 5E and F) which remained high for 4 hours then decreased progressively with time. However, the red fluorescence was significantly above background when the cells were analysed 4 days after labelling. The cell viability, assessed by light scatter, was reduced by approximately 15% post staining, but the remaining viable cells had incorporated the dye. Cell viability recovered with time in culture and the red fluorescence was retained in the viable cell population. Coculturing of labelled cells with an unlabelled cell population indicated that the dye is capable of diffusing between the cells after 24 hours in culture (data not shown). These data suggest that these probes may be useful for whole cell labelling in some flow cytometric applications and would suffer little interference from compounds such as haemoglobin that absorb strongly at lower wavelengths. Under the conditions used for flow cytometry (dual illumination with 488 and 633nm light), there was no significant fluorescence emission recorded in the green

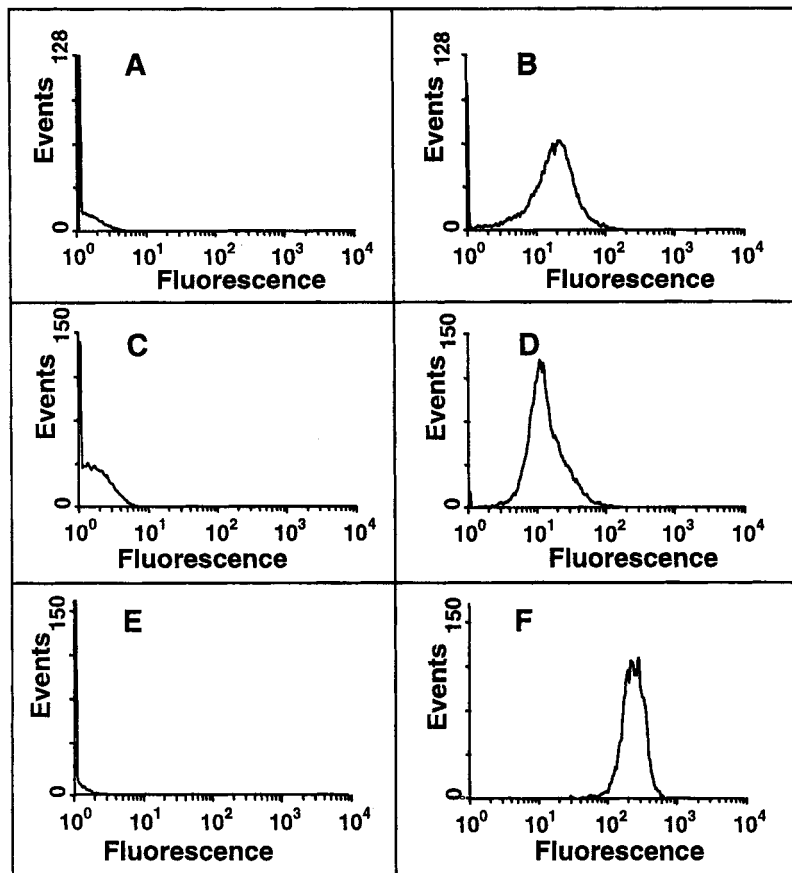


Fig. 5. Flow cytometric analysis. 2,10-DPAPD was added to erythrocyte ghosts (B) intact erythrocytes (D) and (F) NS-1 myeloma cells to achieve a final molar ratio of about one probe molecule per 100 lipid molecules. Flow cytometric analysis was performed using excitation from a 10mW He-Ne laser at 633nm with fluorescence detection at 675nm. Data collection was triggered from the forward angle light scatter signal and red cell fluorescence was gated on the main population of particles detected by light scatter. A, C, E: unlabelled preparations of ghosts, intact erythrocytes and NS-1 cells, respectively.

fluorescence channel (525nm) or the orange fluorescence channel (575nm) even when the cells were heavily loaded with 2,10-DPAPD.

Confocal fluorescence microscopy of 2,10-DPAPD-labelled erythrocyte ghosts and NS-1 myeloma cells was performed using the 647 nm line of a krypton-argon laser. Only membrane-associated probe was visualised with both cell types, although some adherent material on the exterior of the NS1 cells appeared to be also labelled (Figs. 6A and B.) The labelling procedure did not cause extensive vesiculation of the erythrocyte ghosts or myeloma cells as judged by comparison with controls labelled with other membrane-associated probes such as ethidium bromide. Labelling of internal cell membranes of NS-1 cells was observed in cells that were obviously damaged, as determined by their morphology under white

light illumination (Fig. 6D). Cell nuclei showed only traces of internal staining.

DISCUSSION

We have prepared a series of methoxy derivatives and examined the effect of substituting this functional group at various positions on the perylene dione chromophore. The 2,10- and 2,12-disubstituted perylene diones possess the most favourable spectral properties with respect to their stability and quantum yield. In addition, the absorption maxima of the compounds are close to the 633 nm line of the He-Ne laser so that this may be used as a light source to efficiently excite the compounds.

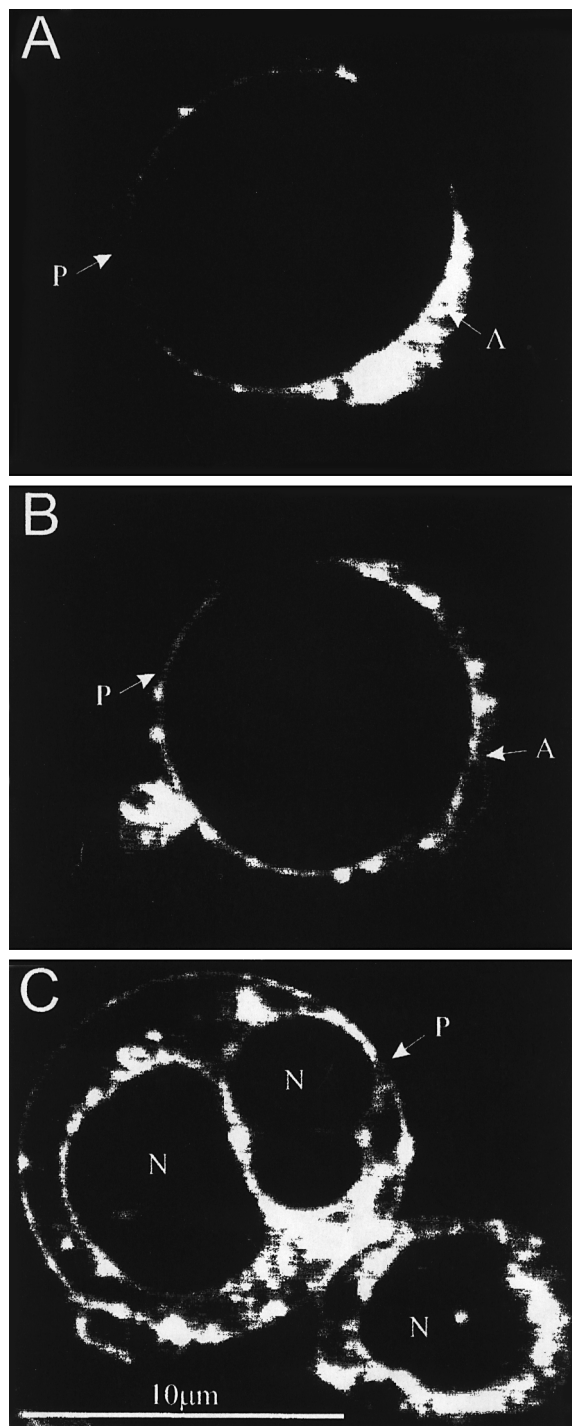


Fig. 6. Confocal scanning microscopy of mouse myeloma (NS-1) cells labelled with 2,10-DPAPD. The cells were labelled as for flow cytometry and observed by microscopy as a suspension in PBS. Optical sections were taken through the median plane of the cells. A, B: Cells showing staining of the plasma membrane and some external cell processes and adherent material. C: Cells with damaged membranes showing staining of interior cell membrane structures. N: Cell nuclei, P: plasma membrane A: adherent material.

The extinction coefficients of the 2,10-disubstituted perylene diones ($23\text{--}30,000\text{ M}^{-1}\text{cm}^{-1}$; Table III) are five to ten fold lower than those of the cyanine dyes [5–8,36]. However, the absorption spectra of the perylene diones are considerably broader (90–120 nm bandwidths; Tables II and III) compared to the cyanine dyes (40 nm bandwidths [5,8]). The perylene dione chromophore could be used with a greater variety of light sources without large sacrifices in the population of molecules excited. In addition, the large spectral bandwidth means there is substantial overlap between the absorption spectrum of the chromophore and the emission spectra of a number of probes which emit in the region of 500–700 nm. The perylene dione chromophore may therefore be useful as an acceptor in applications involving fluorescence resonance energy transfer where the efficiency of transfer may be monitored by the quenching of the donor fluorescence.

The perylene diones exhibit much greater Stokes shifts ($> 60\text{ nm}$) compared to the cyanine dyes (20 nm [5,8]). As a result, a larger proportion of their emission can be collected using appropriate filters without problems arising from scattering artifacts. However, the broad emission spectrum of the compounds could represent a disadvantage in multi-colour applications in immunofluorescence microscopy and flow cytometry.

The perylene diones exhibit a large fluorescence in chloroform but are less fluorescent in the other solvents examined (Table III). Although 2,10-DMPD is not fluorescent in PBS, the weak fluorescence exhibited by 2,10-DPPD and the DNA conjugate, both representing more “water-soluble” forms of the chromophore, suggests that the chromophore may have some weak fluorescence in PBS when it is not in an aggregated form. The presence of little or no fluorescence in water severely limits the application of perylene diones as fluorescent labels in macromolecules. Indeed, both the IgG and DNA conjugates exhibit little fluorescence even in the presence of detergent.

The diphosphate perylene dione derivative has potential applications as a substrate for alkaline phosphatase. The spectral properties of 2,10-DPPD and its hydrolysed product, 2,10-DHPD, are not optimal for use in assays based on chromogenic substrates, however, the perylene dione chromophore has the advantage of being less susceptible to interference from other absorbing and fluorescing compounds when compared to the commonly used chromogenic substrates such as PNPP.

The 2,10-DMPD and 2,10-DPAPD perylene dione derivatives possess a number of properties which would make them useful as membrane probes. The compounds (i) spontaneously associate with membrane structures; (ii) possess a reasonable quantum yield when they are

associated with these structures but are not fluorescent in water; (iii) absorb and emit in the far red region so measurements are less susceptible to scattering artefacts or to other absorbing compounds such as haemoglobin which absorb strongly at lower wavelengths; (iv) have a large limiting anisotropy (> 0.27); and (v) are less susceptible to photobleaching in a lipid environment compared to Cy5.5.

In a flow cytometry application, labelled erythrocyte ghosts, intact erythrocytes and mouse myeloma cells were very readily distinguished from the background signal following excitation of the membrane-embedded probe with a He-Ne laser at 633 nm. Labelling with the dyes did not appear to adversely affect the viability of NS-1 myeloma cells and the fluorescence intensity observed with these cells was much greater than that of erythrocytes, as a result of their greater size. The small degree of cell death observed during the staining procedure could be attributed to the effects of extended incubation in the saline solution. The dye was readily taken up into the cell membranes and appeared to be stably associated with the cells. The reduction of cellular fluorescence observed with time after labelling can be accounted for by some loss from diffusion of the dye out of the cell membranes but also from dilution as the cells replicated and produced unlabelled membrane. In a confocal microscopy application, labelled cells were conveniently visualised by excitation of the membrane-embedded probe using the 647 nm line of a krypton-argon laser. No fluorescence was observed from the probe population in the aqueous phase.

In conclusion, the novel far red fluorophores described in this work have spectroscopic properties which may be useful in a number of biological applications, in particular applications involving flow cytometry, confocal microscopy and measurements of membrane fluidity. These perylene dione chromophores may be particularly useful for samples which contain haemoglobin or other absorbing compounds that could interfere with fluorescence measurements.

ACKNOWLEDGMENTS

This work was supported by the Cooperative Research Centre for Diagnostic Technologies, Australia. The authors wish to thank Dr. Michael Foley and Professor Nick Hoogenraad, Department of Biochemistry, La Trobe University, for useful discussions and Dr. Alan Hibbs, Centre for Molecular Biology and Medicine, Epworth Hospital, Melbourne, Australia, for assistance with some of the confocal fluorescence microscopy studies.

REFERENCES

1. G. Patonay and M. D. Antoine (1991) *Anal. Chem.* **63**, 321A–327A.
2. R. B. Thompson. (1994) in J. R. Lakowicz (Ed.), *Topics in Fluorescence Spectroscopy. Vol. 4. Probe Design and Chemical Sensing*, Plenum Press, New York, pp. 151–181.
3. T. Imasaka, A. Tsukamoto, and N. Ishibashi (1989) *Anal. Chem.* **61**, 2285–2288.
4. T. Imasaka and N. Ishibashi (1990) *Anal. Chem.* **62**, 363A–371A.
5. P. L. Southwick, L. A. Ernst, E. W. Tauriello, S. R. Parker, R. B. Mujumdar, S. R. Mujumdar, H. A. Clever and A. S. Waggoner (1990) *Cytometry* **11**, 418–430.
6. R. B. Mujumdar, L. A. Ernst, S. R. Mujumdar, C. J. Lewis, and A. S. Waggoner (1993) *Bioconjugate Chem.* **4**, 105–111.
7. D. B. Shealy, M. Lipowska, J. Lipowski, N. Narayanan, S. Sutter, L. Strekowski, and P. Patonay (1995) *Anal. Chem.* **67**, 247–251.
8. L. A. Ernst, R. K. Gupta, R. B. Mujumdar, and A. S. Waggoner (1989) *Cytometry* **10**, 3–10.
9. A. E. Boyer, M. Lipowska, J.-M. Zen, G. Patonay, and V. C. W. Tsang (1992) *Anal. Lett.* **25**, 415–428.
10. A. S. Waggoner, L. A. Ernst, and R. B. Mujumdar (1993) U.S. Patent No. 5,268,486.
11. V. T. Oi, A. N. Glazer, and L. Stryer (1982) *J. Cell Biol.* **93**, 981–986.
12. G. P. Anderson, K. A. Breslin, and F. S. Ligler (1996) *ASAIO J.* **42**, 942–946.
13. B. Ballou, G. W. Fisher, T. R. Hakala, and D. L. Farkas (1997) *Biotechnol. Prog.* **13**, 649–658.
14. C. Cullander C (1994) *J. Microsc.* **176**, 281–286.
15. P. B. Sargent (1994) *Neuroimage* **1**, 288–295.
16. P. M. Lansdorp, C. Smith, M. Safford, and L. W. Terstappen (1991) *Cytometry* **12**, 723–730.
17. R. Schmidt, W. Drews, and H.-D. Brauer (1980) *J. Am. Chem. Soc.* **102**, 2791–2797.
18. Th. Blumenstock, F. J. Comes, R. Schmidt, and H.-D. Brauer (1986) *Chem. Phys. Lett.* **127**, 452–455.
19. J. Motoyoshiya, T. Masunaga, D. Harumoto, S. Ishiguro, S. Narita, and S. Hayashi (1993) *Bull. Chem. Soc. Jpn.* **66**, 1166–1171.
20. H.-D. Brauer and R. Schmidt (1983) *Photochem. Photobiol.* **37**, 587–591.
21. K. Hirakawa, E. Ogiue, J. Motoyoshiya, and T. Kakurai (1987) *Bull. Chem. Soc. Jpn.* **60**, 2292–2294.
22. R. Schmidt, W. Drews, and H.-D. Brauer (1982) *J. Phys. Chem.* **86**, 4909–4913.
23. L. Deady, A. Hughes, I. Mahadevan, N. H. Quazi, and L. Tilley (1999) *Synth. Commun.* **30**, 803–820.
24. A. Zouni, R. J. Clarke, A. J. W. G. Visser, N. V. Visser, and J. F. Holzwarth (1993) *Biochim. Biophys. Acta* **1153**, 203–212.
25. S. R. Meech and D. Phillips (1983) *J. Photochem.* **23**, 193–217.
26. N. J. L. Roth and A. C. Craig (1974) *J. Phys. Chem.* **78**, 1154–1155.
27. L. Tilley and G. B. Ralston (1984) *Biochim. Biophys. Acta* **790**, 46–52.
28. W. West and S. Pearce (1965) *J. Phys. Chem.* **69**, 1894–1903.
29. R. Y. Tsien and S. B. Hladky (1978) *J. Membr. Biol.* **38**, 73–97.
30. A. S. Waggoner, C. H. Wang, and R. L. Tolles (1977) *J. Membr. Biol.* **33**, 109–140.
31. Z. Huang, N. A. Olson, W. You, and R. P. Haugland (1992) *J. Immunol. Methods* **149**, 261–266.
32. J. M. Roberts, S. L. Jones, R. R. Premier, and J. C. Cox (1991) *J. Immunol. Methods* **143**, 49–56.
33. J. Suurkuusk, B. R. Lentz, Y. Barenholz, R. L. Biltonen, and T. E. Thompson (1976) *Biochemistry* **15**, 1393–1401.
34. B. R. Lentz, Y. Barenholz, and T. E. Thompson (1976) *Biochemistry* **15**, 4521–4528.
35. K. R. Thulborn, L. Tilley, W. H. Sawyer, and F. E. Treloar (1979) *Biochim. Biophys. Acta* **558**, 166–178.
36. P. J. Sims, A. S. Waggoner, C.-H. Wang, and J. F. Hoffman (1974) *Biochemistry* **13**, 3315–3330.